SOLID-STATE ACTUATION AS A DRIVING MECHANISM FOR MINIATURE SPACECRAFT

Y. 13ar-Cohen, S.-S. Lih,
Jet Propulsion Laboratory, California institute of Technology, Pasadena, CA 91109

and

N. W. Hagood IV
Aeronautics and Astronautics, MI'I', Cambridge, MA 02139

ABSTRACT

Piezoelectric rotary motors are being developed to form a drive mechanism for robotics, miniature spacecraft instruments and subsystems. The technology that has recently emerged in commercial products is associated with empirical design. An analytical model was developed for the motor and it is currently being modified to account for the effect of space environment. The interface between the rotor and stator components anti the friction forces are invest igated to determine the propelling effect of the stator. The model predicts motor performance and can be used to optimize the design of miniature high-torque motors.

NOMENCLATURE

$\boldsymbol{T}$	reduced stress tensor
$\boldsymbol{D}$	electric displacement vector
$\boldsymbol{S}$	reduced strain tensor
$\boldsymbol{E}$	electric field vector
c^E	stiffness constants
e	electromechani cal constants
ε	the dielectric permittivity constant
$\boldsymbol{M}$	mass matrix of the stator
$\boldsymbol{C}$	damping matrix of the stator
$\boldsymbol{K}$	stiffness matrix of the stator
$\boldsymbol{p}$	model amplitude vector
$\boldsymbol{F}_N$	external normal force vector
$\boldsymbol{F}_T$	external tangential force vector
θ	elect romechanical coup] ing constant
V	applied voltage
α	relation angle of the rotor
w_f	rotor flexture height in z direction
I_{rotor}	rotor inertia
C_α	rotor spin damping
τ_{in}	interface torque
$\tau_{applied}$	applied torque
M_{rotor}	rotor mass
C_z	rotor vert i cal damping
F_{int}	interface force
$F_{applied}$	applied for ce

INTRODUCTION

The recent NASA effort to reduce the size and mass of future spacecraft is straining the specifications of actuation and articulation mechanisms that drive robots and planetary instruments. The miniaturization of conventional electromagnetic motor is limited by manufacturing constrains anti lower efficiency. Generally, these types of motors compromise speed for torque using speed reducing gears. The use of gears adds mass. volume and complexity as wc]] as

reduces the system reliability due to the increase in number of the system components. Potentially, rotary piezoelectric motors can offer an effective alternative drive mechanism for miniature instruments [1]. These motors provide high torque density at low speed, high holding torque [2], simple construction, quiet operation and have a quick response. Theycan also be made in annular shape for optical application, electronic packaging and wiring through the center. Piezoelectric motors, also known as ultrasonic motors (USM) arc now being considered for actuation of a robotic arm for a Mars Lander robotic program. A joint JPL/MIT study is underway to develop such motors for operation at space environment, namely, to operate effectively and reliably ina vacuum andat temperatures down to cryogenic levels.

Ultrasonic motors [1-11] can be classified by their mode of operation (static or resonant), type of motion (rotary or linear) and shape of implementation (beam, rod, disk, etc.). Despite the distinctions, the fundamental principles of solid-state actuation tie them together: microscopic material deformations (usually associated with piezoelectric materials) arc amplified through either quasi-static mechanical or dynamic/resonant means. The motor mechanism is based on rectification of the stator wave cyclic motion to drive the rotor in a controlled direction.

Several USM classes have seen commercial application in areas needing compact, efficient, intermittent motion [12, 13]. Such applications include: camera auto focus lenses [14, 15], watch motors [16] and compact paper handling [7]. A comparison of the performance characteristics of rotary electric motors employed in current space applications and USMs is shown in Table 1. The motors, characteristics arc given with no gear reduction and highlight the inherently higher torque density of USMs. To obtain similar levels of torque-speed characteristics with conventional motors, a gear system is added to reduce the speed, thus increasing the size, mass and complexity of the drive mechanism. Piezomotors arc fundamentally designed to have a high holding force, providing effectively zero backlash. The number of components needed to construct a motor is small minimizing the number of potential failure points. The general characteristics of USMs make them attractive fm robotic applications where small, intermittent motions are required.

in Figure 1 the operation principle of solid state ultrasonic motors (traveling wave ring-type motor) is shown as an example. A travel ing wave is established over the staler surface, which behaves as an elastic ring, and produces elliptical motion at the interface with the rotor. This elliptical motion of the contact surface propels the rotor and the drive- shaft connected to it. The teeth, which arc attached to the stator, arc intended to increase the moment arm to amplify the speed. The operation of USM depends on friction at the interface between the moving rotor and stator and it is a key issue in the design of this interface for extended lifetime.

PRINCIPAL OF OPERATION

The general concept of a solid state motor is to produce gross mechanical motion through the amplification and repetition of micro-deformations of active material. The active material induces an orbital motion of the stator at the rotor contact point and frictional

interface between the rotor and stator rectifies the micro-motion to produce macro-motion of the staler as shown in Figure 1. The active material, which is a piezoelectric wafer in this study, excites a traveling bending wave within the staler that leads to elliptical motion of the surface particles. Teeth are used to enhance the speed that is associated with the propelling effect of these particles. The rectification of the micro-motion at the interface is provided by pressing the rotor on top of the stator and the frictional force between the two causes the rotor to spin. This motion transfer between the stator and rotor is similar to a gear action and it leads to much lower rotation speed than the wave frequency.

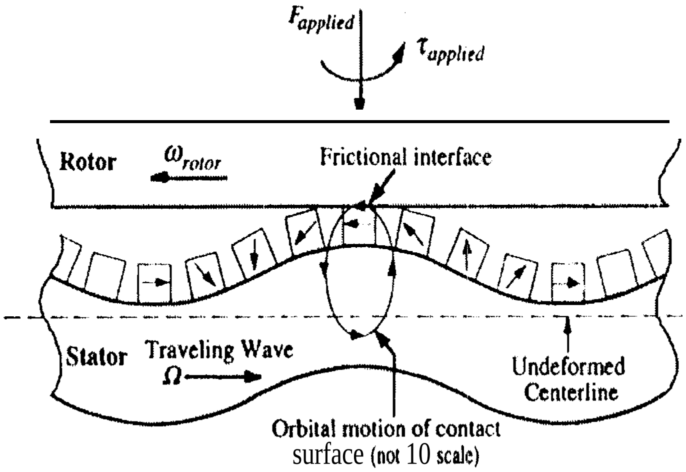

Figure 1. Principle of Operation of a Rotary 'J'raveling Wave Motor (Ring type) [12].

A generic description of the stator is shown in Figure 2. The stator can be driven by a piezoelectric wafer that is placed either on one surface [15] or sandwiched between two wafers [17]. To generate traveling wave, the piezoceramic driver internal poling is structured such that quarter wavelength out-of-phase is formed. This poling pattern is also intended to eliminate extension in the stator and maximize bending. The teeth on the stator arc arranged in a ring at the radial position. in Figure 2 the solid lines indicate permanent etching on the electrode in two groups (A &B). Dashed lines indicate segments that wi 11 be etched for poling purposes and then reconnected with silver paint to reduce the number of leads required. The dark areas arc regions on the piezoelectric wafer that arc not activated. In operation A and B electrodes arc driven 90° out of phase and produce orthogonal disk modes.

To generate a traveling wave within the stator two orthogonal modes arc controlled. These modes arc formed by the piezoceramic poling pattern A of $cos(4\theta)$ and B of $sin(4\theta)$. Geometrical examination of this pattern shows that if the A piezoceramic driver is induced by a $cos(\omega t)$ and B by $sin(\omega t)$, a traveling wave is formed with the frequency of $\Omega = \omega/4$ frequency. Also, by changing the sign cm one of the drive signals, the traveling wave reverses its direction.

THI ;OI<l;r'lCAl/.h401")111_,ING

To *a priori* predict rotary ultrasonic motors the transient and steady state performance an analytical model [17] was developed and a summary will be given herein. The model consists of four sections as illustrated in Figure 3 and is described below. The model sections address the major components that arc responsible for the motor operation, i.e. stator, rotor, interface and motor performance.

'l'All],11 1: Comparison of existing electromagnetic motors (EMM) and ultrasonic motors (USM)

#	Type	Description	Manuf.	Stall Torque (in. oz)	No-load Speed (rpm)	Mass (g)	Torque Density without gear (Nm/kg)
1	EMM	DC, Brushless	Aeroflex	1.4	4.0K	256	0.04
2	EMM	DC Brush	Maxon	1.8	6.0K	38	0.45
3	EMM	AC, 3-phase	Astro	10.7	11.5K	340	0.21
4	USM	Traveling Wave - Disc	Panasonic [12]	11	0.8K	70	1.10
5	USM	Stand. Wave - Rod Torsion	Kumada [8]	189	0.12K	150	8.80
6	USM	Traveling wave - Disc	Shinsei [20]	13	0.3K	33	2.70
7	USM	Traveling wave -Ring	Canon [14]	17	0.08K	45	2.30

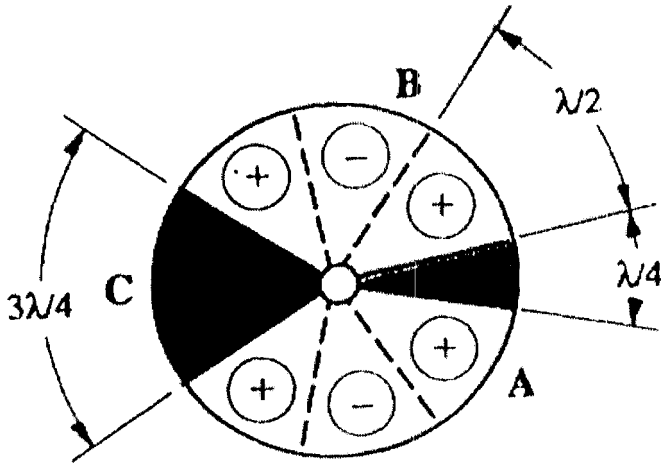

Figure 2: Generic stator design describing the poling sequence on the piezoelectric wafer.

In Figure 3 the analytical model is drawn in the form of a flowchart with the four sections. The Stator Model (Section A) is a dynamic model of a circularly symmetric variable cross section disk. The disk is subject to distributed piezoelectric forces as well as distributed normal and tangential frictional interface pressures caused by motion dependent rotor- stator contact. '1 'he model includes traveling wave motion through temporally and spatially out-of-phase forcing of 90° orthogonal disk modes ass] lown in Figure 4.

In the Interface Mode] (Section 11), a distributed frictional interface is assumed for the contact area between the rotor and stator, see Figure 4. This provides for modeling the rotor-stator contact compliance and allows distributed normal and tangential forces at the contact surface. The Rotor Model (Section C) assumes a rigid body dynamic model of the rotor motion (vertical and horizontal/rotary). It assumes an externally applied normal force and torque as well as motion-dependent interface forces that are derived from rotor-staler contact.

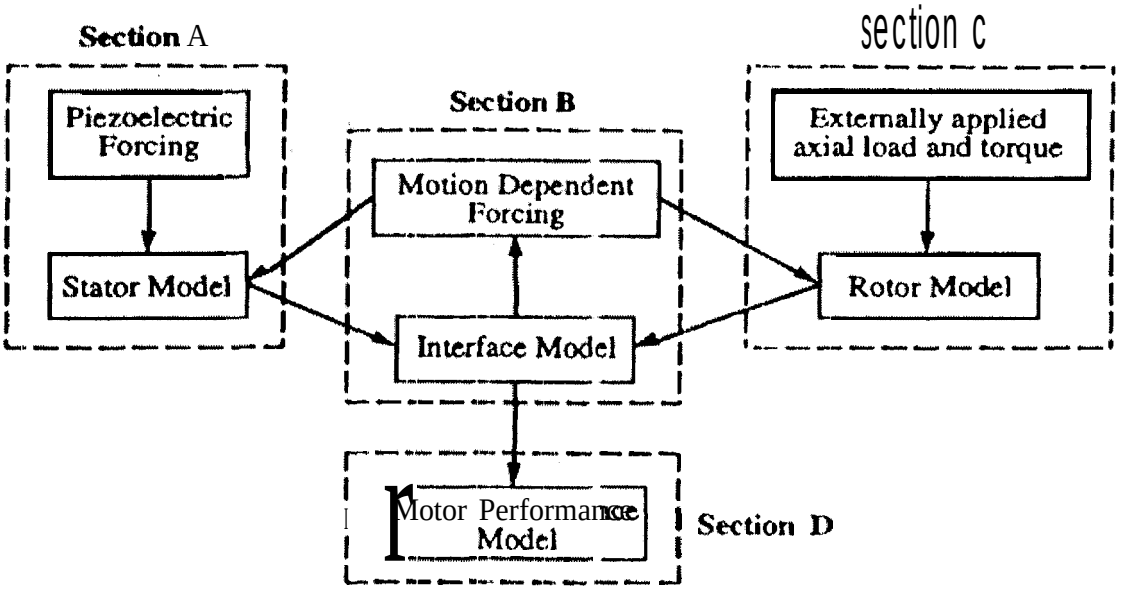

Figure 3: Modeling approach consists of major motor components which are: stator, rotor, interface, and motor performance.

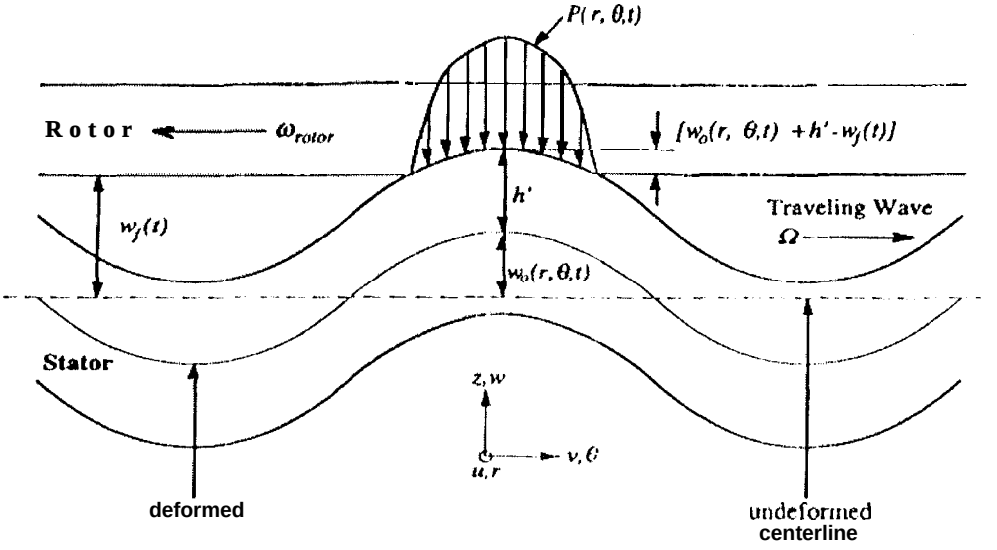

Figure 4: Model for interface between the rotor and stator. Distributed horizontal frictional force is not shown.

The Motor Performance Model (Section D) provides a performance prediction module using transient or steady stale values of rotor position and velocity to calculate positioning accuracy and steady state mechanical power output, It calculates the current input into piezoelectric electrodes using a fully coupled electromechan ical model. Using the current and the known applied voltage it calcul atcs average electrical power input and efficiency.

The piezoelectric constitutive equation in the model used can be expressed as

$$\begin{bmatrix} \boldsymbol{D} \\ \boldsymbol{T} \end{bmatrix} = \begin{bmatrix} c^{T} & e \\ -e^{T} & c^{E} \end{bmatrix} \begin{bmatrix} \boldsymbol{E} \\ \boldsymbol{S} \end{bmatrix}$$

where $\boldsymbol{T}$ is the stress tensor in reduced form, $\boldsymbol{D}$ is the electric displacement vector, $\boldsymbol{S}$ is tbc strain tensor in reduced form, and $\boldsymbol{E}$ is the electric field vector. The definitions of the st i ffness constants c'", the electromechanical constants c, and tbc dielectric permittivity constant c can be found in [17]. The governing equation for tbc rotor can be written as

$$\boldsymbol{M}\ddot{\boldsymbol{p}} + \boldsymbol{C}\dot{\boldsymbol{p}} + \boldsymbol{K}\boldsymbol{p} = \Theta V + \boldsymbol{F}_N + \boldsymbol{F}_T$$

where $\boldsymbol{M}, \boldsymbol{C}$ and $\boldsymbol{K}$ arc the mass, damping and stiffness matrices of the stator, respectively, and $\boldsymbol{p}$ is the mode] amplitude vector. $\boldsymbol{F}_N$ and $\boldsymbol{F}_T$ arc the external normal and tangential force vectors, Θ is the eletromechanical coupling constants and V is the applied voltage.

The rotor is modeled by equations of motions decoupled in the rotary direction by the rotation angle α and in the z direction by the flexture height w_f (the distance between tbc undeformed stator height and the rotor lower surface). 1 lence, the rotation equation can be expressed as

$$I_{rotor}\ddot{\alpha} + C_{\alpha}\dot{\alpha} = \tau_{int} - \tau_{applied}$$

where I_{rotor} is the rotor inertia, C_{α} is tbc rotor spin damping, and τ_{int} and $\tau_{applied}$ is the interface torque and applied torque respectively. The equation of the rotor in the z direction can be expressed as

$$M_{rotor}\ddot{w}_f + C_z\dot{w}_f = F_{int} - F_N$$

where M_{rotor} is the rotor mass, C_z is the rotor vertical damping, F_{int} and $F_{applied}$ arc the interface force and applied forces, respectivel y. 1 3y solving the rotor and stator equations, the performance of the motor can thus be evaluated, and details of tbc calculation can be found in [17] and arc omitted here for brevit y.

ANALYSIS OF PIEZOELECTRIC MOTORS

The analysis of the nonlinear, coupled rotor-stator d ynamic model d i scussed above has demonstrated the ability to predict the motor transient and steady state performance as a function of critical design parameters. 'J'best parameters include characteristics such as the interface normal force, tooth height and stator radial cross section. Steady state motor performance data have been generated including the speed-torque curves and efficiency-torque curves for

various parameters such as teeth height and interface forces [17].

The model was computer coded and was used to simulate the motor response as a function of various design parameters. This simulation has indicated the critical role of the motor factors in determining its efficiency and power output. 11 also has shown that current motor designs operate well under their peak potential performance due to limitations on interface pressure imposed by lifetime issues related to wear at the rotor/stator interface.

A simulation of the motor response to an applied force input $F_{applied}$ and torque $\tau_{applied}$ alone and the inertia and damping terms were evaluated for various values from no-load to stall level. It was determined that the modal amplitude increases from zero until tile normal and tangential work terms begin to take energy out of the stator subsystem. After several oscillations a steady state is reached. At the initial phase a negative term appears due to the applied axial load which must be balanced by the interface force to be zero both initially and at steady state, The rotor, modeled as a flexure, must therefore deform to accommodate the interface force. These oscillatory response al the transient phase can be controlled by the motor electronic driver to minimize this overshoot.

Two factors dominate the optimization of the motor performance: the tooth height anti the applied axial loading. Analysis of the motor performance has shown that an increase of the teeth height increases the speed of the motor with relatively small effect on the stall torque. Further, the effect of the teeth height on the motor efficiency requires optimization since there is an increase at small values reaching a maximum at certain ratios of the teeth height to the stator thickness.

The two most important characteristics of the motor are speed-torque and efficiency - torque. Evaluation of these graphs for low axial loading yields a low stall torque and a relatively fast no-load speed. As the axial loading increases, a steady state progression is observed from high no-load speeds and low stall-torques to lower no-load speeds and high torque. 'The rotor speed decrease is due to the normal forcing on the stator, as the axial load increases, more energy is taken out of the stator vibration and thus the stator surface velocity decreases which in turn affects the rotor velocity. Examination of the efficiency-torque curves is showing that maximizing the output power does not maximize the efficiency. The cause of this behavior is the clamping effect that is associated with the increased load and reduced capability of the stator to resonate.

'To optimize the motor efficiency a parametric study was initiated. The materials that are used to produce the stator and rotor have important effect on the motor performance. 'The key motor parameters that were used in the calculations are:

Stator:

Materials: aluminum/brass
Outer disk radius: 3 cm
Inner hole radius: 2.23 cm
Thickness: 0.24 cm

Rotor

Material: bronze
Mass: 0.05 kg
Inertia: 0.00001 kg-m^2
Flexural stiffness: $2e^{12}$ N-m^2
c_o: $2e^{-6}$ N-m-S
C_r: 500 N-s/m

Piezoelectric element:

Material: PZT-4
d_{31}: -1 10 C-12 m/v
Clamped dielectric: 1550 ϵ_0
Thickness: 0.051 cm

Interface Material:

Material: Kapton
Young's modulus: 2.85 Gpa
Poisson's ration: 0.35
1 Dynamic coefficient of friction: 0.32

A set of speed-torque curves were produced for aluminum, bronze and steel and are shown in Figure 5. The curves in Figure 5 indicate that an aluminum stator produces the highest speed-torque response for the above set of selected parameters. Further, the stall torque is not affected by the choice of the stator/rotor material. This parametric study is being pursued toward optimization of the motor design parameters. 1 urther, efforts are currentl y directed towards the inclusion of the effect of temperature and vacuum.

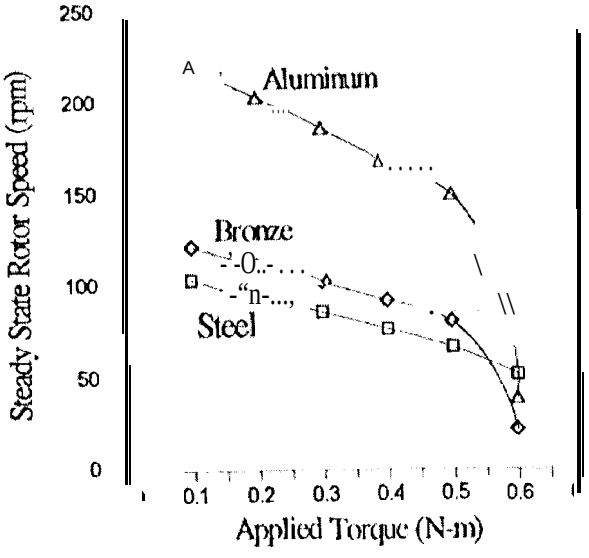

Figure 5: Motor performance curves.

CONCLUSIONS

A parametric study of the motor model that account for the effect of the friction at the stator-rotor interface provided a valuable insight into the mechanical and dynamics of how piezoelectric motors operates. The model presented can be used to optimize the operation of piezoelectric motors including the effect of the teeth and the applied axial loading for maximum performance.

ACKNOWLEDGMENT

'1 he research described in this paper was performed under a contract with the National Aeronautics and Space Administration. It is part of a larger task on Mars Lander robotics (1'.1., 1 Dr. Paul Schenker, JPL). The goal of this task is to advance mechani sins, cent rols and machine intelligence for next generation planetary in-situ science exploration.

The authors would like to thank Mr. Dion Manly for his assistance in the parametric study. Mr. Manly is a Summer Technical Intern at JPL and a student at University of California, Irvine.

REFERENCES

1. J. M.] Hollerbach, 1. W. 1 lunter and J. Ballantyne, "A Comparative Analysis of Actuator Technologies for Robotics." in Robotics Review 2, MIT Press, Edited by Khatib, Craig and Lozano-Perez (1991).
2. ,4. Flynn, "The Scoop on Ultrasonic Motors in Japan," Office of Naval Research Asian Office Scientific Information Bulletin, NAVSO 1'-3580,

Vol. 17, No. 2,April-.luI]c,(1992) pp. 99-102.
3. Burleigh Instruments Product Catalogue, Burleigh Instruments, Inc. Fishers, New York.
4. "The Application of Terfenol in Linear Motors Development," Proc. 2nd International Conf. Giant Magneto-strictive and Amorphous Alloys for Sensors and Applications, (1 988) pp.1-118.
5. J. M. Vranish, 1). 1'. Naik, J.S. Restorff and J.P. Toter,"Magnetostrictive 1 Direct 1 Drive Rotary Motor," IEEE Trans, on Msg., Vol. 27, No, 6, (Nov. 1991) p 5335.
6. K. Uchino, K. Kato and M. Tohda, "Ultrasonic Linear Motors Using a Multilayered Piezoelectric Actuator," Ferroelectrics, Vol. 87, pp. 331-334, 1988.
7. 'I'. Inoue, S. Takahashi and M. Suga, "Application of Ultrasonics to Paper Transport Mechanisms," Techno, (May, 1989) pp. 4749, in Japanese,
8. A, Kumada, "A Piezoelectric Ultrasonic Motor," Japanese Journal of Applied Physics, Vol. 24, Supplement 24-2, pp. 739-741, (1 985).
9. R. J. Zemella, "Design and Development of a Linear Traveling Wave Motor, " Ml']' Master's Thesis in Aeronautics and Astronautics. (May 1990).
10. K. Minoru, S. Ueha, and E. Moru, "1 Excitation Conditions of Flexural '1'raveling Waves for a Reversible Ultrasonic Linear Motor," Journal of the Acoustic Society of Japan, Vol, 77, No. 4, (April 1983).
11. R. Inaba, A. Tokushima, (), Kawasaki, Y. Ise, and 11. Yoneno, "Piezoelectric Ultrasonic Motor," Proceedings of the 11 IEE Ultrasonics Symposium, pp. 747-756, (1981).
12. " Ultrasonic Motor", Panasonic Technical Reference. Panasonic industrial Co., 1 Division of Matsushita Electric Corp. of America, 1Panasonic Way, Secaucus, NJ, (1987).
13. Y. Masaki, "Vibrator and Ultrasonic Motor 1 Employing the Same," U. S. Patent 4,983,874, January 8, (1991).
14. K. Hosoe,"An Ultrasonic Motor for Use in Autofocus 1 Lens Assemblies," Techno. pp. 36-41, May,1989, in Japanese.
15. "Cannon Develops an 11 x25-mm Miniature Ultrasonic Motor," Cannon, Nikkei Mechanical, (June 1, 1992).
16 "Seiko Ultrasonic Micromotor Data Sheets", Seiko Instruments Inc., I'recision Instruments Department, (Consumer Products Div., 1-9-1 Miyakubo, Ichikawa-shi, Chiba 272, Japan, (1 99?).
17. N. W. Hagood and A. McFarland, "Modeling of a Piezoelectric Rotary Ultrasonic Motor," IEEE Transactions on Ultrasonics, Ferroelectrics and 1 requency Control, Vol. 42, No. 2, 1995 pp. 210-224.